Demonstration of Berry's Phase Using Stored Ultracold Neutrons

D. J. Richardson
Institut Laue-Langevin, BP-156X, 38042 Grenoble CEDEX, France

A. I. Kilvington and K. Green
Rutherford-Appleton Laboratory, Chilton, Didcot, Oxfordshire, OX11 0QX, United Kingdom

S. K. Lamoreaux[(a)]
Physics Department, FM-15, University of Washington, Seattle, Washington 98195
(Received 30 June 1988)

Using stored spin-polarized ultracold neutrons subjected to a temporally varying magnetic field, we have demonstrated a manifestation of Berry's phase. We verified several properties of Berry's phase which include its solid-angle dependency and additivity for multiple excursions along the same path in parameter space.

PACS numbers: 03.65.Bz, 28.20.−v, 33.25.−j, 35.20.My

As first recognized by Berry,[1] when the dynamics of a quantum system are governed by a Hamiltonian H which is described by a multidimensional parameter, if that parameter is varied adiabatically around a closed curve C in parameter space, the system will return to its original state apart from a circuit-dependent phase factor $e^{i\gamma(C)}$ in addition to the usual dynamical phase $\exp[-i\int H(t)dt]$. This phase factor is known as Berry's topological phase and has simple form when the system is nearly degenerate: $\gamma(C)\propto\Omega(C)$, where $\Omega(C)$ is the solid angle that C subtends at the degeneracy (origin) of the parameter space. In particular, for spins in a magnetic field $\mathbf{B}$ which is varied such that the tip of $\mathbf{B}$ traces out a closed curve during a time interval T, $\gamma_m(C) = -m\Omega(C)$, where m is the spin component along $\mathbf{B}$ (see Sec. 4 in Ref. 1). This phase appears in addition to the dynamical phase $\phi_m=\kappa m\int_0^T B(t)dt$, where κ is the gyromagnetic ratio.

We have experimentally tested Berry's theory using spin-polarized stored ultracold neutrons subjected to a slowly varying magnetic field. Our results complement a recent test by Bitter and Dubbers.[2] In our experiment, we vary the magnetic field in time while spatially confining the neutrons. With our technique, in addition to verifying the solid-angle dependency, we were able to demonstrate that $\gamma(C)$ is additive for multiple excursions along the same path, that "ellipticity" (to be defined) does not affect the outcome, and that the neutron has a negative magnetic moment.

We varied the magnetic field in the neutron storage volume as follows: For $0\le t\le NT$,

$$B_x=\alpha B_0 \text{ for } \epsilon=0 \quad =0 \text{ for } \epsilon\neq 0, \qquad (1)$$
$$B_y=\pm(1+\epsilon)B_0\cos 2\pi t/T\,,\quad B_z=B_0\sin 2\pi t/T\,,$$

and $B_x=B_y=0$, $B_z=B_z^0$ for all other times. The neutron polarization initially pointed along z. N is the number of rotations of the magnetic field vector, T is the time for one rotation, B_0 is the length of the magnetic field vector, ϵ is the ellipticity parameter which allows the magnitude of B to be varied over the path [the projection of the tip of $\mathbf{B}$ traces out an ellipse in the y-z plane; this parameter is used only in the case of $\Omega(C)=2\pi$], and α is used to vary the solid angle: $\Omega(C)=2\pi(1\pm\cos\theta)$, where θ is the apex angle of the cone described by $\mathbf{B}$ and $\cos\theta=\alpha/(1+\alpha^2)^{1/2}$, and the $\pm$ sign depends on the rotation direction and sign of the magnetic moment. All of the parameters were each independently adjustable.

For spin-$\frac{1}{2}$ particles (e.g., neutrons), Berry's analysis shows that in addition to the dynamical phase

$$\phi_\pm=\pm\tfrac{1}{2}\kappa\int_0^T B(t)dt \quad (=\pm\kappa B_0T \text{ for } \epsilon=\alpha=0)\,,$$

there will be an additional phase (in the adiabatic limit) $\gamma_\pm(C)=\mp\Omega(C)/2$, where the $\pm$ sign refers to the $s=\pm\frac{1}{2}$ spin states of the neutrons. We define the polarization as $P_z=|a_+|^2-|a_-|^2$, where the neutron spin state is described by $\psi=a_+|+\frac{1}{2}\rangle+a_-|-\frac{1}{2}$, and $|a_+|^2+|a_-|^2=1$. The neutrons are initially in the $+\frac{1}{2}$ state, thus $\psi(0)=|+\frac{1}{2}\rangle$ and $P_z(0)=1$. If we assume that the direction of the magnetic field is constant, the time-dependent Schrödinger equation is readily solved for $0<t<T$ with the result $\psi(T)=\cos\phi_+|+\frac{1}{2}\rangle -i\sin\phi_-|-\frac{1}{2}\rangle$. Berry's analysis shows that if the direction of the magnetic field is varied over a closed path, we must also include the circuit dependent phase $\gamma_\pm(C)$ which must be added to the dynamical phase; this yields the result

$$P_z(T)=\cos^2[\phi_++\gamma_+(C)]+\sin^2[\phi_-+\gamma_-(C)]$$
$$=\cos 2[\phi_++\gamma_+(C)]\,,$$

since $\phi_++\gamma_+(C)=-[\phi_-+\gamma_-(C)]$.

Berry's analysis is most easily understood in the context of the present experiment by solving Schrödinger's equation for the case $\epsilon = 0$. For a system of noninteracting spin-$\frac{1}{2}$ particles, the solution is the same as for a classical magnetic dipole.[3] If one transforms into a frame rotating about $\hat{\mathbf{x}}$ at $t=0$, that is, where $\mathbf{B}$ ($B_{x'} = \alpha B_0$, $B_{y'} = B_0$, and $B_{z'} = 0$) is constant, an additional field is generated along $\hat{\mathbf{x}}$, giving $B_x = \alpha B_0 \mp 2\pi/\kappa T$ where the $\mp$ sign refers to the rotation direction. The neutrons are initially polarized along $\hat{\mathbf{z}}$ and the spins simply precess about the quadrature sum of the fields and $P_{z'} = \cos[\kappa (B_{x'}^2 + B_{y'}^2)^{1/2} t]$. At $t = T$, the rotating and laboratory frames coincide: $P_{z'}(T) = P_z(T)$. Thus, the final neutron polarization is given by

$$P_z = \cos\{[(\kappa B_0 T)^2 + (\alpha \kappa B_0 T \mp 2\pi)^2]^{1/2} - 2\pi\}, \quad (2)$$

where the -2π is necessary so that the total phase $\Phi = 0$ when $B_0 = 0$. The total field in the laboratory frame is $B = B_0(1+\alpha^2)^{1/2}$. In the adiabatic limit ($\kappa B T \gg 1$), the total phase is

$$\Phi = \kappa B T - 2\pi \left[1 \pm \frac{\kappa}{|\kappa|} \frac{\alpha}{(1+\alpha^2)^{1/2}} \right]$$
$$= \phi - \Omega(C) = \phi + \gamma(C), \quad (3)$$

where $\gamma(C) = 2\gamma_+(C)$, which is exactly as predicted by Berry's analysis. For multiple rotations, the total time is NT and the phases in Eq. (3) are simply multiplied by N. Thus, for multiple rotations, Berry's phase is additive as expected. Note that since we are not having the neutron wave functions interfere but are only manipulating the spin quantum number, we are not sensitive to spinor rotation effects.[2,4]

Ultracold neutrons (UCN) are neutrons which have a velocity of about 5 m/s or less. If the Fermi potential of a material surface is high enough, UCN will be reflected from that surface with negligible probability of loss for all neutron incident angles.[5] If a bottle is made of such a material and if the surface contaminants can be kept low enough, UCN can be stored for a time limited only by the decay of the neutron.[6] We use a bottle made of Be and BeO both of which have high Fermi potentials; however, in this bottle the neutron storage lifetime is limited to 80 s by surface contaminants (probably hydrogen)[7] and by leaks in the valve which is used to fill and empty the bottle. In addition, UCN propagate in pipes made of high Fermi potential materials (e.g., stainless steel) in a manner similar to that of low-density gas.

A schematic of our experiment is shown in Fig. 1. We used the neutron electric-dipole-moment measurement apparatus which has been fully described elsewhere[8-10] with the addition of a third coil so that a magnetic field can be applied along any axis within the magnetic shield. We will now briefly describe the experiment.

UCN are generated at the Institut Laue-Langevin high-flux reactor as follows.[11] Both UCN and very cold neutrons (VCN) originate in a 25-l liquid-deuterium cold source (25 K). The UCN and VCN are transported through a nickel coated guide which has a 10-m vertical rise and then through a turbine which further slows down the VCN and doubles the available UCN density. The UCN density at the turbine output is $\approx 90\ n/\text{cm}^3$.

As shown in Fig. 1, UCN from the turbine pass along a stainless-steel guide to an 0.8-μm magnetically saturated Co-Ni polarizing foil. The polarized UCN transmitted by the foil pass along a Cu-Ni alloy coated silica guide through holes in the large five-layer Mumetal magnetic shield into a 5-l storage volume which consists of two 25-cm-diam polished Be plates separated 10 cm by a sintered BeO cylindrical insulator. (The high-voltage components of the electric-dipole-moment apparatus are unused in this experiment and can be ignored.) The neutron polarization is initially along a 5-mG field in the z direction. After filling the bottle for about 10 s the neutron density approaches its maximum value of about $10\ n/\text{cm}^3$ and the neutron valve is closed. After waiting 2 s to allow the system to equilibrate, the polarized neutrons are subjected to a temporally varying magnetic field over a time $T = 7.387 \pm 0.005$ s followed by another 2-s wait. The neutron valve is then opened and the neutrons are counted as follows. The polarizing foil now acts as an analyzer for the z component of the neutron spin. An adiabatic spin flipper allows both spin states to be counted. While the neutrons were being stored, the input guide was switched to now divert the neutrons to a ^{3}He proportional counter. Each spin state is counted for 10 s.

The magnetic field is generated by the use of three sets of coils within the magnetic shield and outside the vacuum vessel. The coils are mutually orthogonal to within 2° and are calibrated to within 0.1%. The currents are generated by an analog computer which is controlled by a timer and zero-crossing switch to provide exactly one or multiples of one rotation. A single control sets B_0 [see Eq. (1)] which greatly facilitates the measurements.

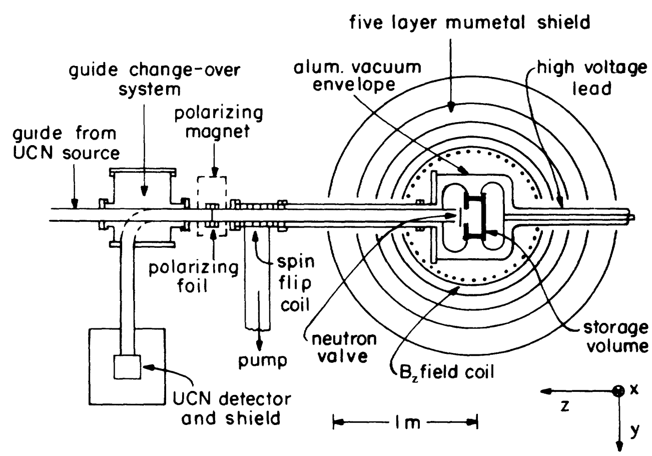

FIG. 1. Schematic of the experimental apparatus. ($B_{x,y}$ field coils are not shown.)

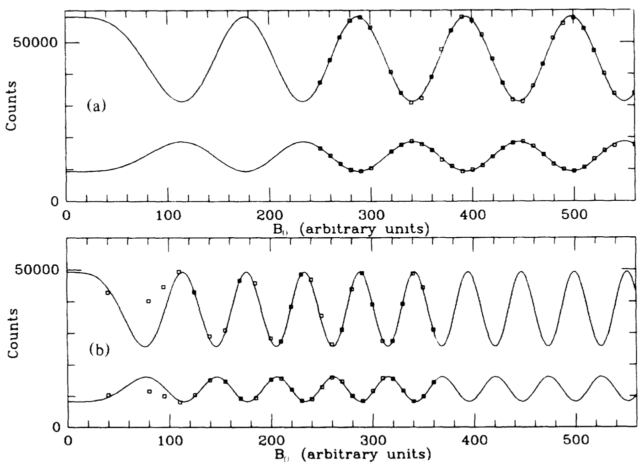

FIG. 2. Spin-up (upper curves in each plot) and spin-down neutron counts as a function of B_0, where $\alpha=0$, $\epsilon=0$, and positive rotation sense. (a) Data for one rotation and (b) data for two rotations. Note the low-field depolarization in (b).

The residual field averaged about 10 μG in the storage vessel with a gradient across the vessel of the same magnitude. At low values of B_0, the neutron spins were depolarized by the residual fields and thus set a lower limit on B_0 and an upper limit on T. This depolarization is evident in Fig. 2(b) for $B_0 < 100$. In addition, there was a lower limit on T because the storage vessel was enclosed in an aluminum can. We had originally set $T \approx 0.5$ s and although the varying field penetrated the can fairly well, the eddy current induced gradients rapidly that depolarized the neutrons. We found that $T \approx 7$ s did not give a significant depolarization at high B_0 and measurements with low B_0 ($\kappa B_0 T/2\pi \approx 1$) were also possible.

For a given set of parameters N, α, and ϵ, the spin-up and spin-down neutron counts were measured as a function of B_0, each datum requiring a fill and store per count cycle rate. Figure 2 shows typical results [$\gamma(C) = 2\pi$]. Note the aperiodicity in the neutron count oscillations near $B_0 = 0$. It is this aperiodicity which leads to the Berry's phase shift in the adiabatic limit.

There are several ways to extract Berry's phase from the data. One is to determine the values of B_0 which give maxima in the spin-up counts; at these points $\Phi = 2\pi n$, where $n = 0, 1, 2, \ldots$ and $n=0$ corresponds to $B_0 = 0$. Although our data does not extend to $B_0 = 0$, we can still unambiguously determine the phase. Our data extends low enough so that at most one oscillation can occur between our lowest B_0 and $B_0 = 0$. Note also that the oscillation period increases as B_0 approaches zero in all cases. We thus miss at most the $n=1$ maximum and its location can be approximately determined.

Instead of measuring only the locations of the maxima, each set of data was also analyzed as follows. The spin-up and spin-down neutron counts vary with the phase Φ as

$$n_{\rm up} = n^0_{\rm up}(1 + p_{\rm up}\cos\Phi)\,,$$
$$n_{\rm down} = n^0_{\rm down}(1 - p_{\rm down}\cos\Phi)\,, \qquad (4)$$
$$\Phi = 2\pi[a_1 x^2 + (a_2 x + a_3)^2]^{1/2}\,,$$

where x is proportional to B_0, $p_{\rm up} \approx p_{\rm down} \approx A^2$ where A is the polarizing efficiency of the polarizer which is also used as the analyzer, and $n^0_{\rm up}$ and $n^0_{\rm down}$ are the average detected number of up-spin or down-spin state neutrons. Φ in Eq. (4) is the most general form of the phase as Eq. (2) indicates. Note that we need not have an accurate calibration of B_0 to determine Berry's phase for the data set; one can readily determine the phase in the adiabatic limit by taking the appropriate combination of the fit coefficients [see Eq. (2)]. Analysis by this technique gives a lower uncertainty on the phase since there are

TABLE I. Results of the Berry's phase demonstration. N is the number of rotations, RS is the rotation sense [the $\pm$ sign in Eq. (1)], $\Omega^{+,-}_{\rm calc}$ is the theoretical value of $\Omega(C)$ for a positive or a negative magnetic moment, and $\Omega^{u,d}_{\rm obs}$ is the measured $\Omega(C)$ from the spin-up (u) or spin-down (d) counts.

α	θ	ϵ	N	RS	$\Omega^{+}_{\rm calc}/2\pi$	$\Omega^{-}_{\rm calc}/2\pi$	$\Omega^{u}_{\rm obs}/2\pi$	$\Omega^{d}_{\rm obs}/2\pi$
0.000	90	0.62	1	+	1.000	1.000	1.01(03)	1.00(05)
0.000	90	0.25	1	+	1.000	1.000	1.00(03)	0.99(05)
0.000	90	0.00	1	+	1.000	1.000	1.00(01)	1.00(02)
0.000	90	−0.50	1	+	1.000	1.000	1.02(03)	0.99(06)
0.000	90	0.00	2	+	2.000	2.000	2.00(03)	1.97(06)
0.000	90	0.00	3	+	3.000	3.000	2.87(15)	2.89(15)
0.268	75	0.00	1	+	0.741	1.259	1.28(01)	1.26(03)
0.577	60	0.00	1	+	0.500	1.500	1.52(02)	1.51(03)
1.000	45	0.00	1	+	0.293	1.707	1.68(01)	1.69(02)
1.000	45	0.00	1	−	1.707	0.293	0.26(02)	0.20(10)
1.732	30	0.00	1	+	0.134	1.866	1.74(15)	1.72(40)
3.732	15	0.00	1	+	0.034	1.966	1.97(01)	1.98(02)
0.577	30	0.00	2	+	1.000	3.000	3.00(03)	2.99(05)

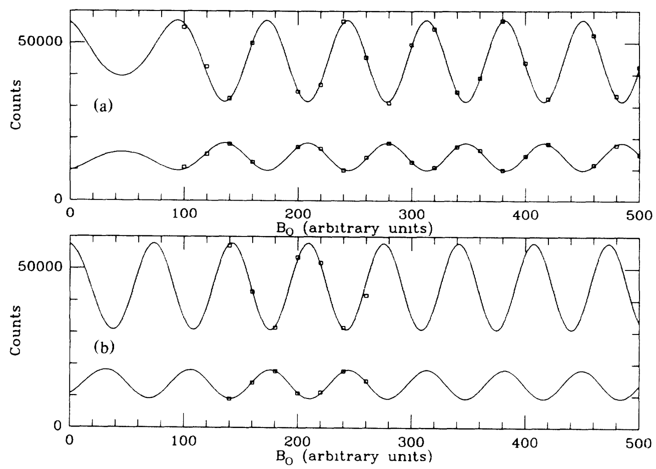

FIG. 3. Neutron counts as a function of B_0 where $\alpha = 1$ ($\theta = 45°$), $\epsilon = 0$; (a) positive rotation sense, (b) negative rotation sense.

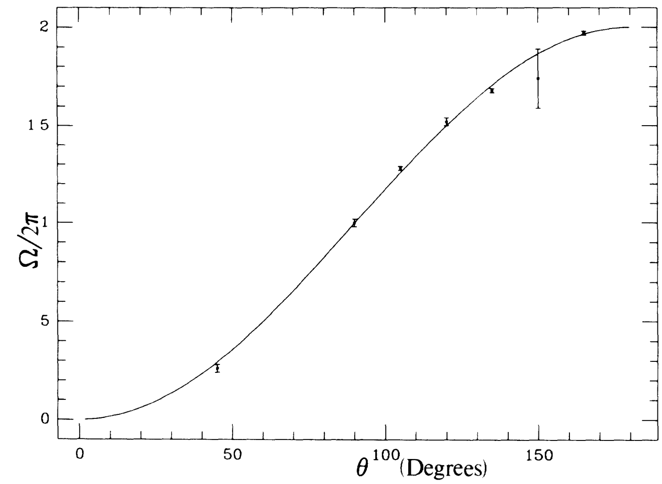

FIG. 4. Expected solid angle (solid curve) as a function of set value of θ compared with the experimental solid angle (points) as determined by Berry's theory.

more points used in its determination than when only the points near the maxima are used.

We found that typically $n^0_{\rm up} \approx 34000$, $n^0_{\rm down} \approx 13000$, and $p_{\rm up} \approx p_{\rm down} \approx 0.5$. p is lower than what is observed in normal operation of the electric-dipole-moment experiment where $p \approx 0.6$. Some loss of polarization probably occurs because the initial field along $\hat{\mathbf{z}}$ which guides the neutron polarization into the bottle is 5 mG as opposed to 10 mG as used in a normal operation. The various coefficients are different between spin up and spin down because the spin-up neutrons are counted first. The spin-down neutrons suffer additional losses in number and polarization as they are stored in the guide and reflect off of the polarizer while the spin-up neutrons are being counted. We thus have separate measurements of Berry's phase from the spin-up and spin-down neutron counts.

Results of the fits to various data sets are tabulated in Table I. χ^2 for the fits varied between 1 and 10 where the uncertainty was taken to be shot noise in the neutron counts. We neglect the error in the setting of B_0 which was significant in the case of multiple rotations and large solid angles. This additional error accounts for larger χ^2. There were probably no contributions from systematic effects at our level of sensitivity. We did not include the data taken at low B_0 because of the residual field depolarization; the effect of the residual fields becomes small rapidly as B_0 increases. Also, the error in the set value of $\Omega(C)$ due to uncertainties in the field calibration was negligible in comparison to the error of $\Omega(C)$ as determined from the fit.

Our results show that Berry's phase is indeed additive and that ellipticity does not affect the outcome to high accuracy. One also sees immediately that the sign of the neutron magnetic moment is $\kappa/|\kappa| = -1$. This is particularly evident in the data in Figs. 3(a) and 3(b) since the oscillations are drawn toward the vertical axis for the positive rotation. Figure 4 is a plot of $\Omega(C)$ vs θ where $\theta \rightarrow 180 - \theta$ for positive rotations since the magnetic moment is negative. Although this additional phase is inherent in Schrödinger's equation and is accounted for by transforming to the rotating frame, Berry's analysis suggests a new way to think about magnetic moments precessing in a varying magnetic field.

The authors thank C. Bouchiat for useful information. We also thank N. F. Ramsey and R. Golub for stimulating discussion in regard to this work, and R. Golub for critically reviewing the manuscript. This work was supported by the United Kingdom Science and Engineering Research Council, by NSF Grant No. PHY-8711762, and by the Institut Laue-Langevin.

---

[a]Visiting scientist from the Institut Laue-Langevin, 38042 Grenoble CEDEX, France.

[1]M. V. Berry, Proc. Roy. Soc. London A **392**, 45–57 (1984).

[2]T. Bitter and D. Dubbers, Phys. Rev. Lett. **59**, 251–254 (1987).

[3]C. Cohen-Tannoudji *et al.*, *Quantum Mechanics* (Wiley Interscience, New York, 1977), pp. 443–454.

[4]*Neutron Interferometry,* edited by U. Bonse and H. Rauch (Oxford Univ. Press, New York, 1979).

[5]R. Golub and J. M. Pendlebury, Rep. Prog. Phys. **42**, 439–501 (1979).

[6]P. Ageron *et al.*, Nucl. Instrum. Methods Phys. Res., Sect. A **249**, 261–264 (1986).

[7]W. A. Lanford and R. Golub, Phys. Rev. Lett. **39**, 1509–1512 (1977).

[8]J. M. Pendlebury *et al.*, Phys. Lett. **136B**, 327–332 (1984).

[9]T. Sumner, Ph.D. thesis, Sussex University, 1979 (unpublished).

[10]P. M. C. de Miranda, Ph.D. thesis, Sussex University, 1987 (unpublished).

[11]A. Steyerl *et al.*, Phys. Lett. A **116**, 347–352 (1986).